Arabian Journal of Chemistry (2022) **15**, 104012

King Saud University

Arabian Journal of Chemistry

www.ksu.edu.sa
www.sciencedirect.com

ORIGINAL ARTICLE

Optimization of biodiesel production via transesterification of soybean oil using α-MoO_3 catalyst obtained by the combustion method

Adriano Lima Silva [a,*], Ana Flávia Felix Farias [a], Simoni Margareti Plentz Meneghetti [b], Edson Antonio dos Santos Filho [c], Ana Cristina Figueiredo de Melo Costa [a]

[a] *Synthesis of Ceramic Materials Laboratory (LabSMaC), Postgraduate Program in Materials Science and Engineering (PPG-CEMat), Academic Unit of Materials Engineering, Federal University of Campina Grande, Av. Aprígio Veloso-882, Bodocongó, 58429-900, Campina Grande, PB, Brazil*
[b] *Group of Catalysis and Chemical Reactivity (GCAR), Institute of Chemistry and Biotechnology, Federal University of Alagoas, 57072-970 Maceió, AL, Brazil*
[c] *Polymer Processing Laboratory (LPP), Postgraduate Program in Materials Science and Engineering (PPG-CEMat), Academic Unit of Materials Engineering, Federal University of Campina Grande, Av. Aprígio Veloso-882, Bodocongó, 58429-900, Campina Grande, PB, Brazil*

Received 17 January 2022; accepted 24 May 2022
Available online 30 May 2022

KEYWORDS

Orthorhombic phase;
Ethyl esters;
Heterogeneous catalysis;
Experimental planning

Abstract A catalyst based on MoO_3 was synthesized by a simple and fast pilot-scale combustion reaction method and applied to the conversion of soybean oil to biodiesel via transesterification. For that, the statistical analysis of the catalyst amount and temperature, factors that influence the process, was evaluated by means of central composite design 2^2. MoO_3 was characterized in terms of structure by X-ray diffraction (XRD), textural characterization Brunauer-Emmett-Teller (BET), density by helium pycnometry (DE), particle size analysis (DG) and acidity tests by temperature-programmed desorption of ammonia (NH_3-TPD), chemical analysis by X-ray fluorescence (EDX), morphology by scanning electron microscopy (SEM) and catalytic properties. The transesterification products were characterized by gas chromatography (GC), acidity index (AI) and kinematic viscosity (KV). The results indicate the catalyst formation with a surface area of 1.36 m^2g^{-1}, and density of 4.5 g/cm^3 which consists of a single crystalline phase of orthorhombic configuration, with total NH_3 acidity of 33.61 μ.mol/g. Morphological characterization revealed

* Corresponding author.
E-mail address: adrianolimadasilva@hotmail.com (A.L. Silva).
Peer review under responsibility of King Saud University.

Production and hosting by Elsevier

https://doi.org/10.1016/j.arabjc.2022.104012

that the catalyst is formed by irregular plates of various sizes and shapes, with a wide sizes range of agglomerated particles. In the soybean oil transesterification reactions, the catalyst was active showing 96.9% conversion to ethyl esters. The experimental design was meaningful and predictive, with a reliability level of 95%. The statistical analysis identified temperature as a significant variable for the adopted planning. To conclude, a new single-phase catalyst (α-MoO_3) has been developed and successfully applied to the biodiesel Synthesis from soybean oil. These results have a positive and promising impact for biodiesel production by transesterification of soybean oil against ethanol.

1. Introduction

Biodiesel is a strong candidate to replace petroleum diesel, since it is one of the green fuels widely studied around the world, in order to reduce the environmental impacts caused by burning fossil fuels, under the aspect of greenhouse gas emissions such as COx, NOx, SOx, CxHy, particulates and other organic compounds that cause global warming (Gonçalves et al., 2021; Santos et al., 2019; Silva et al., 2020a; Silva et al., 2020b). It is a biofuel chemically composed of fatty acids monoalkyl esters, which can be obtained by transesterification and/or esterification of animal or vegetable oils and fats, as well as their rejects in the presence of a catalyst (Santos et al., 2019). In biodiesel production, heterogeneous catalysis may be very important in order to optimize the production process giving greater economic viability and thus making it more sustainable (Xie and Wang, 2020). In this context, research has focused on the use of solid catalysts in order to minimize some of the problems faced by classical homogeneous catalysts (Xie and Wang, 2020; Santamaria et al., 2021; Xie and Wan, 2019).

Among the solid heterogeneous catalysts reported in the literature, MoO_3-based oxides have drawn the attention of the scientific community due to their wide application (Xie and Wang, 2020; He et al., 2018; Gadamsetti et al., 2018; Sangeetha et al., 2019), with prominence in catalysis for biodiesel production because it has Lewis and Brønsted-Lowry acid sites that can lead to high conversions (Santos et al., 2019; Xie and Wan, 2019). Recent work describes the use of MoO_3 applied in biodiesel production, generally being used as an active phase supported on other materials: $MoO_3/SrFe_2O_3$ (Gonçalves et al., 2021), MoO_3/Al_2O_3 (Navajas et al., 2020), MoO_3/CeO_2 (Shadidi et al., 2020), MoO_3/ZrO_2/ KIT-6 (Wang et al., 2022) and others (Xie and Wan, 2019; Chandar et al., 2019; Maniruzzaman et al., 2014; Ramos et al., 2019). However, its use as a mass active catalyst (unsupported), is poorly reported, being found only the recent works of the researchers Pinto et al. (Pinto et al., 2019) and Silva et al. (Silva et al., 2022), which report the application of MoO_3 as a mass catalyst in biodiesel production.

Regarding the synthesis methods of MoO_3, it has been obtained by several techniques: hydrothermal (Nagyne-Kovacs et al., 2020; Sen et al., 2019), microwave (Sangeetha et al., 2019), aqueous solution (Song et al., 2017), wet chemistry (Chandar et al., 2019), solid-state decomposition (Muthamizh et al., 2020), pyrolysis (Baez-Rodriguez et al., 2019), electrochemical pyrolysis (Dighore et al., 2016), sol–gel (Al-Alotaibi et al., 2021); Pechini (Pinto et al., 2019) and the combustion reaction (Silva et al., 2022; Shahsank et al., 2021), even though it is rarely reported in the literature among the existing techniques, is considered a method that has advantages. The combustion reaction is classified as a relatively simple, fast, easy, effective and low-cost method, besides being consolidated in the literature as a procedure used in the preparation of several oxides with application in biodiesel production (Silva et al., 2020a; Silva et al., 2020b; Farias et al., 2020).

In this context, obtaining and applying molybdenum trioxide-based catalysts that meet the premises of economic and environmental benefits, as already mentioned (Song et al., 2017; Muthamizh et al., 2020), the present study highlights as its objective the use of experimental planning techniques, which are widely used as optimization strategies for industrial processes, as they allow an insight into the influence of multivariable involved in industrial and research productions and experiments (Navajas et al., 2020; Farias et al., 2020; Ali et al., 2015; Mushtaq et al., 2021). The experimental planning presents itself as a valuable resource to simulate real situations of the industrial day-to-day life, enabling the projection of a significant reduction of costs and energy expenditures (Gonçalves et al., 2021; Silva et al., 2020b).

The optimization of biodiesel synthesis conditions, is a technique widely applied and reported in the literature (Silva et al., 2020a; Silva et al., 2020b; Farias et al., 2020), as reported by Gonçalves et al. (2021), who evaluated the reaction conditions of the catalytic application of MoO_3 supported on $SrFe_2O_3$ in the production of biodiesel from waste oil, but the authors studied severe synthetic variables and obtained ~95.4% methyl ester conversions in 4 h of reaction, alcohol:oil molar ratio of 40:1, 10% catalyst dosage.

In this context, the objective of this work was to use a factorial design composed of central and axial points to optimize the reaction conditions and evaluate the catalytic capacity of an acid catalyst (MoO_3 obtained by pilot scale combustion reaction) in the ethyl transesterification of soybean oil.

2. Materials and methods

2.1. Materials

To obtain molybdenum trioxide (MoO_3) by combustion reaction, the following reagents were used: ammonium heptamolybdate (HMA) - $(NH_4)_6Mo_7O_{24}{\cdot}4H_2O$ (99%, Sigma-Aldrich – USA); nitric acid - HNO_3 (65%, Nuclear – Brazil); urea - $CO(NH_2)_2$ (98%, Dinâmica – Brazil).

For the catalytic tests were used ethyl alcohol (99%, Dynamic - Brazil) and refined soybean oil (brand SOYA) purchased at a local store. The oil showed fatty acid composition typical of soybean oil (12 % of palmitic acid (16:0), 4 % of stearic acid (18:0), 18 % of oleic acid (18:1), 54 % of linoleic acid (18:2), and 12 % of linolenic acid (18:3)).

2.2. Methods

For the Synthesis of the MoO_3-based catalyst, by combustion reaction, high purity reagents were used with reaction initial solution composition was based on the total valence of the oxidizing and reducing reagents using concepts from the chemistry of propellants and explosives (Jain et al., 1981). In this context, ammonium heptamolybdate $(NH_4)_6Mo_7O_{24}$ $4H_2O$) was used as a metal precursor to obtain MoO_3, being the molybdenum (Mo) and oxygen (O) were considered as oxidizing elements and urea ($CO(NH_2)_2$) was considered a reducing agent (fuel).

The valences of the reactive elements are C = +4; H = +1; N = 0, O = −2 and Mo = +6 (Jain et al., 1981). For a maximum energy release, the stoichiometric coefficient of the com-

position of the reaction mixture was considered (Φe = 1), where the entire all the oxygen content of the metal precursor must oxidize, leading to an equilibrium of zero oxygen (OB = 0) (Hwang et al., 2005).

The mixtures of precursor reagents were carried out by magnetic stirring in a stainless steel container that makes up the conical reactor belonging to the pilot plant (Costa and Kiminami, 2012), coded P08 with a production capacity of 20 g. Then the pH was controlled (2–5) and stirring was maintained for about 20 min, being later taken to the combustion system in the pilot plant, Fig. 1 (a). The synthesis of MoO_3 by combustion reaction performed on different days and times and the calculated for obtain 10 g of product. Based on chemical reaction of theoretically balanced MoO_3 synthesis, expressed by Eq. (1):

$$2[(NH_4)_6Mo_7O_{24}](aq) + 4H_2O(aq) + 6[CO(NH_2)_2](aq) \rightarrow \mathbf{14MoO_3(s)} + 18NH_4(g) + 4H_2O(g) + 6CO_2(g) + 3\ N_2(g) \quad (1)$$

So, considering a 1:1 stoichiometry (1 mol of Mo corresponds to 1 mol of MoO_3), the Synthesis requires an equivalent amount of "n" moles of fuel that the synthesis of 10 g requires for Φe = 1 was calculated, therefore: 0.005[7x(-6) + 24x(-2) + nx(+6)] = 0, n = 0.03/6 = 0.005 mol of urea).

For the synthesis in the pilot plant (Fig. 1a), two heating systems were used, differentiated by the reactor heating source (adapted System I - composed of a belt-shaped heating element attached to the stainless steel container and superimposed on a spiral heating element; and the patented System II - composed of a heating mantle on the side and at the base, to which the stainless steel container is attached). Two circular lateral resistances were added to both systems, with the purpose of keeping the temperature free from external interference, as illustrated in Fig. 1(b).

Five reactions were performed, distributed according to the use of the heating systems: Reactions (1) and (3) using System I, and reactions (2), 4, and 5 using System II. Subsequently, the synthesized samples were mixed using a pitcher mil (ACB - LABOR), and the sample designated as α-MoO_3, sieved in

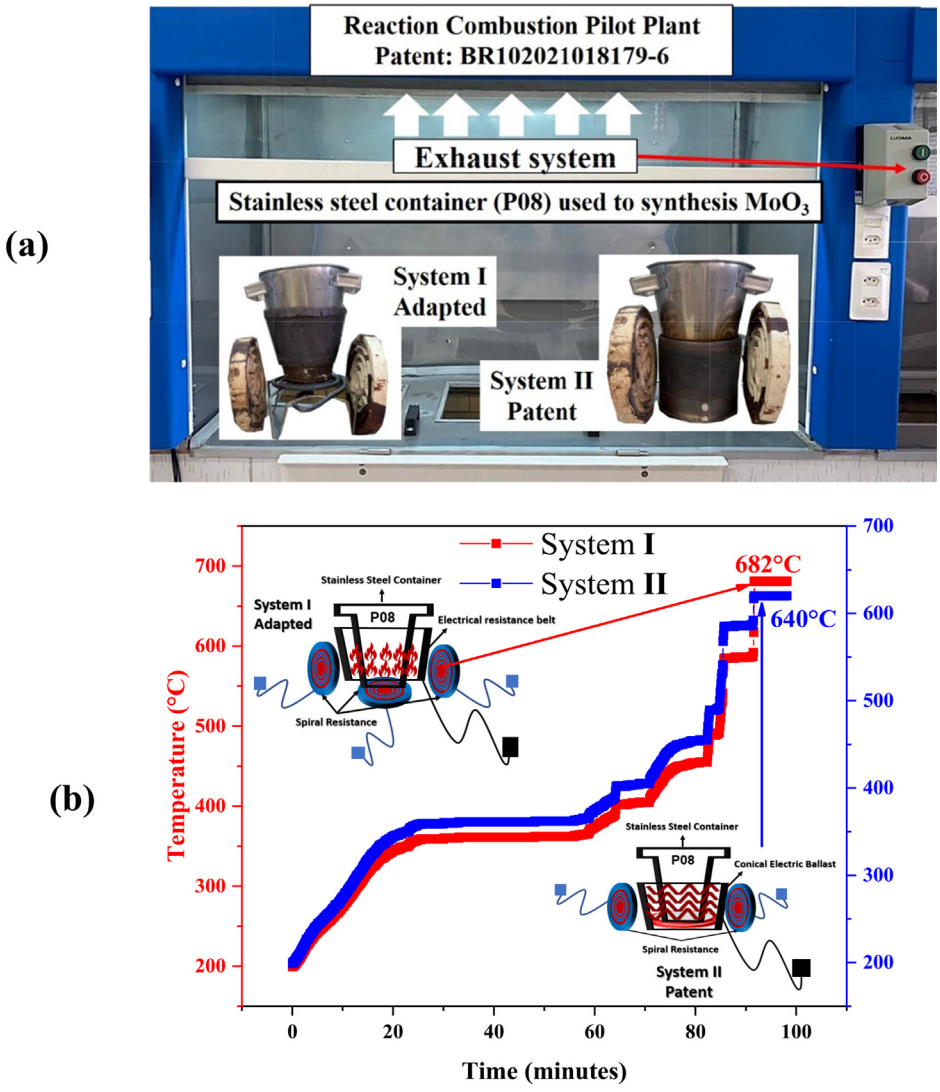

Fig. 1 (a) Combustion reaction pilot plant; (b) Heating system used in the combustion reaction Synthesis of MoO_3.

ABNT 200 mesh (44 μm) and then characterized structurally, morphologically and tested catalytically.

2.3. Catalytic test

The α-MoO_3 catalyst performance was evaluated in the Synthesis of biodiesel in duplicate using soybean oil via transesterification reaction. The catalytic tests were conducted in a pressurized system stainless steel reactor (Parr 4848), with a capacity of 100 mL, mechanical stirrer, time and temperature controller and pressure indicator. The fixed experimental conditions used were: 30 g of oil, time 60 min, alcohol/oil proportion (15:1) and 600 rpm of stirring. The temperature and he percentage of catalyst (concerning the oil mass) were evaluated as variables of the experimental design discussed in the topic: Statistical Analysis, next. After the reaction, the products of the catalytic tests, purified (with warm distilled water) and dried in an oven at 110 °C for 30 min with manual stirring at 5 min intervals.

2.4. Statistical analysis

For the biodiesel synthesis process optimization from soybean oil, a 2^2 factorial experimental design with star configuration and central points was developed, totaling 4 central point trials and 12 randomized experiments. Table 1 describes the input levels and variables for the proposed experimental design.

The two levels for the selected factors were determined from preliminary experiments and with the help of recent published literature (Pinto et al., 2019; Lima and Perez-Lopez, 2018). From the choice of variables and levels, the planning matrix was obtained (Table 2), with the help of *Statistic 7.0* software, which was used for the analysis of the experiments through the level curves, the ANOVA table and the Pareto chart.

The soybean oil conversion into biodiesel (Y) was used as the response to determine the optimized parameters. The effect of independent factors on dependent factors was analyzed by a quadratic equation (2), following the suggested star configuration for the proposed planning.

$$Y = \alpha 0 + \Sigma_{i=1}^{k} \alpha iXi + \Sigma_{i=1}^{k} \alpha iiX^2 i + \Sigma_{i<1}^{k} \alpha ijXiXj + e \quad (2)$$

In which: Y is the response variable to ester content; α0 is the response at the Center point; αi is the first-order linear coefficient; αij is the linear coefficient of interaction between variables; αii is the second-order coefficient and e refers to the pure error associated with the experiments, Xi and Xj are input variables.

Table 1 Proposed variables and input levels for central composite experimental planning 2^2.

	Levels				
Variables	**−1.41**	**−1**	**0**	**+1**	**+1.41**
Temperature (°C)	79.3	100	150	200	220.7
Catalyst concentration (%)	1.6	2	3	4	4.4

* Fixed conditions: 30 g oil mass, time 1 h, and alcohol/oil ratio (15:1).

Table 2 Factorial design 2^2 matrix for the catalytic testing experiments.

Experiments	Temperature (°C)	Catalyst (%)
1	−1	−1
2	−1	+1
3	+1	−1
4	+1	+1
5	−1.44	0
6	+1.44	0
7	0	−1.44
8	0	+1.44
9 (C)	0	0
10(C)	0	0
11(C)	0	0
12(C)	0	0

2.5. Characterizations

The combustion reaction temperature was measured on-line at a time interval of 5 s between each measurement, according to the calibration of the device and its recording software. For this procedure an infrared pyrometer was employed (Raytek, model RAYR3I ± 2 °C). The time of the combustion Synthesis was measured using a digital chronometer (Technos brand).

The α-MoO_3 catalyst was characterized by X-ray diffraction (XRD) using a BRUKER X-ray diffractometer (model D2 PHASER, Cu-Kα radiation), operating with 30 kV and 10 mA, with copper Kα radiation source ($k\alpha$ = 1.54056 Å). The sweep range used at 2θ = 10° at 70°, with an angular step of 0.016° and a counting time of 1.000 s per step. The crystalline phases identification were carried out from the ICDD crystallographic records of the PDF2 / 2019 database with the aid of *DiffracPlus* Suite Eva software, which was also used to obtain the crystallinity values and the size of the crystallite (calculated with the aid of the Scherrer equation) (Klug and Alexander, 1974).

Thermogravimetric analysis (TGA/DTA) was evaluated using a Shimadzu TA 60H simultaneous thermal analysis system, with heating rate 12.5 °C/min under air atmosphere 100 mL/min (maximum temperature 1000 °C).

The surface of the catalyst was characterized using the nitrogen gas adsorption and desorption technique. All experiments were performed using Quantachrome equipment, model AutosorbIQ. The surface area was calculated using the Brunauer, Emmett and Teller (BET). The actual density value the of catalyst (α-MoO_3), was obtained through the analysis in Quantachrome Corporation Upyc 1200e v5.04 Pycnometer, operating with helium gas (He).

The semi-quantitative analysis of the oxides and elements present in the samples were determined by energy dispersive X-ray fluorescence spectroscopy, model EDX-720, from Shimadzu.

The laser diffraction particle size analysis uses the liquid phase particle dispersion method associated with an optical measurement process through laser diffraction on the Mastersizer 2000 equipment from Malvern.

The morphological aspects of the catalyst sample were acquired by scanning electron microscopy (SEM), brand Tescan, model Vega3.

The acidity of the catalyst was determined through desorption analysis at the programmed ammonia temperature (TPD-NH_3) and measurements were performed using a Termolab multipurpose analytical system (SAMP3). For these measurements, approximately 100 mg of the sample were deposited in quartz wool, and the consumption of the gases was measured with a thermal conductivity detector (TCD). Approximately 100 mg of sample was pretreated at 400 °C under a helium atmosphere (30 mL.min^{-1}). Then, the temperature was reduced to 100 °C, and the sample was subjected to ammonia current, for chemical adsorption, for 45 min. In the final step of the adsorption process, NH_3 molecules were removed at 100 °C for 1 h and helium flow rate 30 mL.min^{-1}. The TPD-NH_3 profiles were obtained on heating (from 100 °C to 800 °C), at 10 °C.min^{-1}, and under a helium flow rate (30 mL.min^{-1}). The number of acid sites considering the superficial area was calculated by dividing the total acidity by the area (S_{BET}).

The percentages of ethyl esters were determined by gas chromatography in a single experiment, according to ASTM-D6584 (American Society for Testing Meterials, 2008), using a chromatograph instrument (VARIAN 450c) with a flame ionization detector (FID) and a capillary column as the stationary phase (Varian Ultimetal "Select Biodiesel Glycerides RG"; dimensions: 15 mm × 0.32 mm × 0.45 mm). The initial injection temperature was 100 °C, the oven temperature was 180 °C, and the detector operated at a temperature of 380 °C. The conversions were calculated using normalizations of the signal areas of biodiesel, mono, di and triacilglycerides.

Acid value (AV) and kinematic viscosity (KV) were determined according to AOCS Cd 3d-63 (AOCS, 2017) and ASTM D445 (American Society for Testing Meterials, 2000), respectively.

3. Results

Fig. 2 is illustrated the time and temperature measurements results of the five Synthesis performed to obtain the α-MoO_3 catalyst during the combustion reaction process. In which it is possible to observe that the Synthesis is possible to identify three distinct stages of combustion.

However, it is possible to observe that the Synthesis 1, and 3, presented similar combustion stages behavior to each other. Stage 1 is characterized by the temperature rise and the moisture evaporation followed by reactants liquefaction. In stage 2, moderate gas release was observed, followed by ignition of the combustion reagents (between 15 ~ 45 min). At this stage, the threshold reached at maximum temperatures was instantaneous of 672 °C and 667 °C, respectively. After this stage, a temperature decay of the combustion system is observed, which corresponds to stage 3 (Fig. 2).

Distinct stages of combustion were obtained for the Synthesis 2, 4 and 5, in relation to the Synthesis 1 and 3, because the first stage is marked by a temperature rise moderate with consequent moisture evaporation and gas release. In stage 2, the maximum temperature level reached was continuous (from 41 min to about 82 min), reaching at ~608 °C and soon after, is observed the temperature decay in stage 3.

This difference in the stages profiles and maximum temperature combustion observed in the Synthesis conducted using the systems I and II, is an indication that in system 1 there

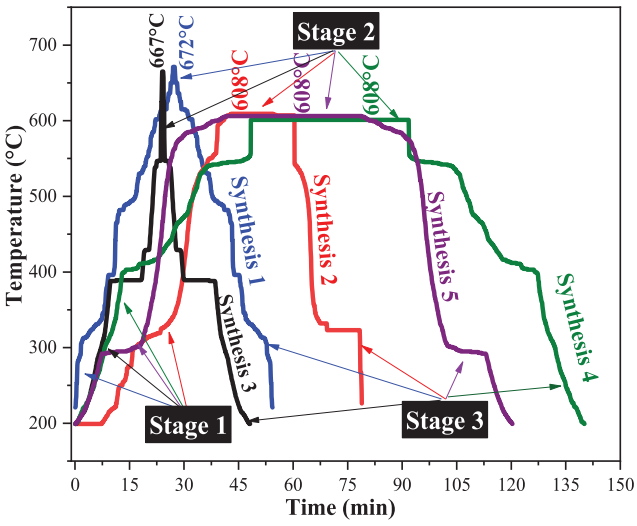

Fig. 2 Behavior (t × T) of combustion reaction measured during the α-MoO_3 Synthesis.

was a greater and faster heat generation than in system II, however, consequently, energy loses at same speed. At the same time, in system II there was less energy loss to the environment, keeping the heat generated for a longer time.

It was also possible to notice that since there is a heat transfer by conduction, convection and radiation to the reaction medium, considering the losses to the environment, the maximum combustion temperatures in the Synthesis are always lower than in the combustion system temperatures (Bergman et al., 2000). The reactions behavior observed is typical of combustion reaction, because it is in consonance with the behavior reported by Dantas et al. (2021), when preparing mixed iron oxides by this method. Table 2 describes the parameters: pH, total time and maximum temperature of the reaction, and the mass yield of α-MoO_3 obtained in each synthesis.

The acid average pH of the precursor solutions to the Synthesis was 3.4, used for favored for the solubilization of precursors. The average reaction time was 88 min, the average mass yield of product from the Synthesis was 9.06 g (90.60%) and the average combustion temperature was 609 °C. In summary, the reaction process for obtaining the α-MoO_3 catalyst was cost-effective, fast and reproducible, since it showed a considerable yield.

In Fig. 3, are illustrated the x-ray diffractograms of the catalyst MoO_3 obtained in the five combustion reaction Synthesis performed.

According to the diffractograms (Fig. 3) it is possible to observe that the products formed in all Synthesis present similar characteristics of orthorhombic crystalline system of MoO3 with ingle phase of high crystallinity, identified by the pattern card PDF2(2019) 00-005-0508. This results also indicate that the proposed catalyst presented good reproducibility, since there was no significant variation in the structural characteristics of the catalyst obtained in different Synthesis systems. With these identifications, the five different Synthesis products were mixed and the obtained sample were named as α-MoO_3, (MoO_3 with Orthorhombic Crystal System) with the intention of simplifying the discussion. The X-ray mixture product diffractogram is shown in Fig. 4, as well as the respec-

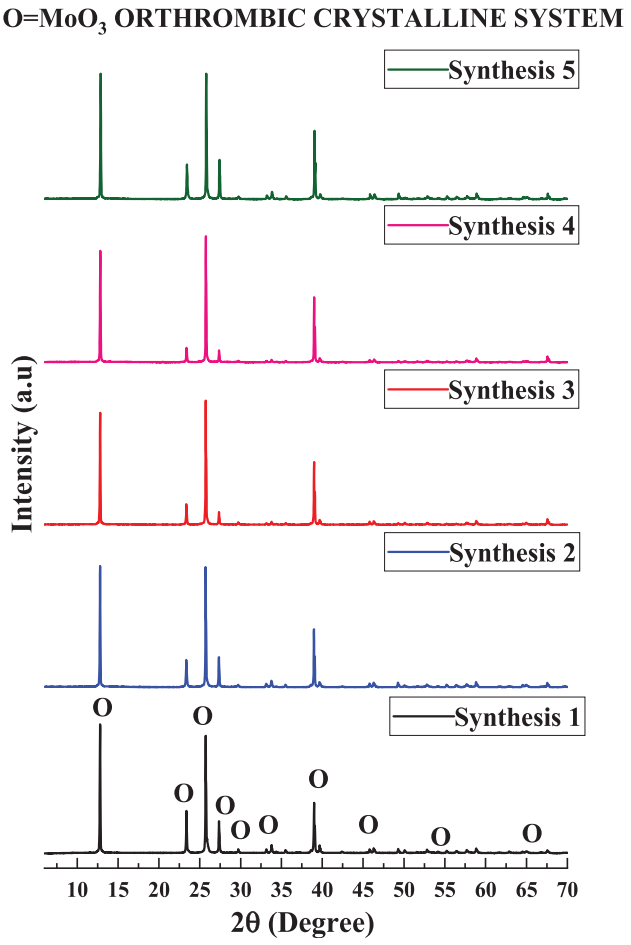

Fig. 3 X-ray diffraction of the five Synthesis by combustion to obtain the catalyst based on MoO_3.

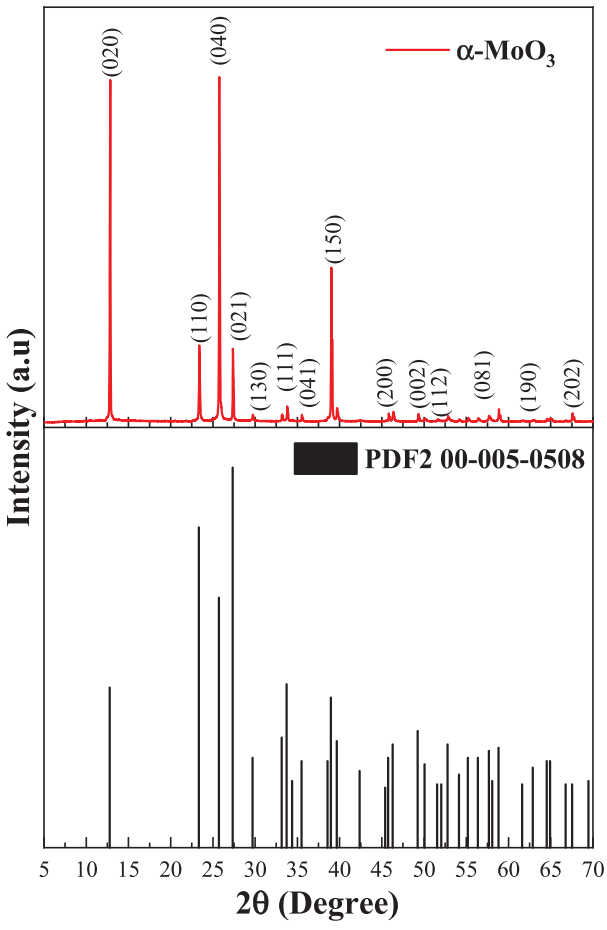

Fig. 4 X-ray diffractogram and pattern card PDF00-005-0508 of the α-MoO_3 catalyst.

tive diffraction planes for the α-MoO3 catalyst sample obtained by combustion reaction.

The x-ray diffraction result of the MoO_3 Synthesis mixture (Fig. 4) confirms what has already been observed in Fig. 3, where the single-phase α-MoO_3 catalyst, was obtained with high purity and with orthorhombic configuration identified by pattern PDF2(2019) 00-005-0508. In addition, it has crystallinity and crystallite size of 90.30% and 80.76 nm, respectively.

The single-phase product obtained in this work stands out in comparison with the recent research of Al-Alotaibi et al. (2021), who in their studies obtained MoO_3 by different Synthesis methods (sol–gel and hydrothermal), using expensive reagents and with calcination after the Synthesis process, at a time of up to 12 h with temperatures ~600 °C. Therefore, the combustion reaction method presented in this paper and in literature recently published by our group (Silva et al., 2022), confirms that the preparation of MoO_3-based catalysts by combustion reaction is promising and economical, since it is a fast process that allows to obtain a highly crystalline and pure single-phase product with proven reproducibility.

Fig. 5 illustrates the thermal events observed in the TGA/DTGA/DTA curves for the catalyst (α-MoO_3), from which the decomposition temperatures (°C) and mass losses (%) could be determined.

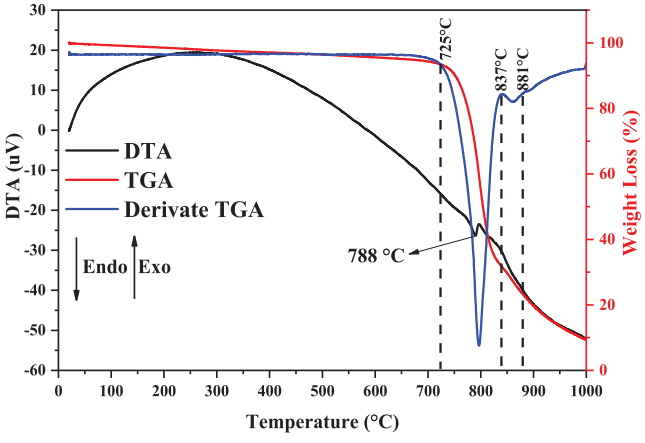

Fig. 5 Overlapped TGA/DTA/Derivate TGA curves for the catalyst (α-MoO_3).

Thermal analysis (TGA) reveals the thermal stability of the catalyst, observed up to temperature 725 °C. Thereafter, the degradation process starts through two mass loss events in the temperature range between 725 and 881 °C, with a total mass loss of 89.68%. The DTA curve for the α-MoO_3 catalyst,

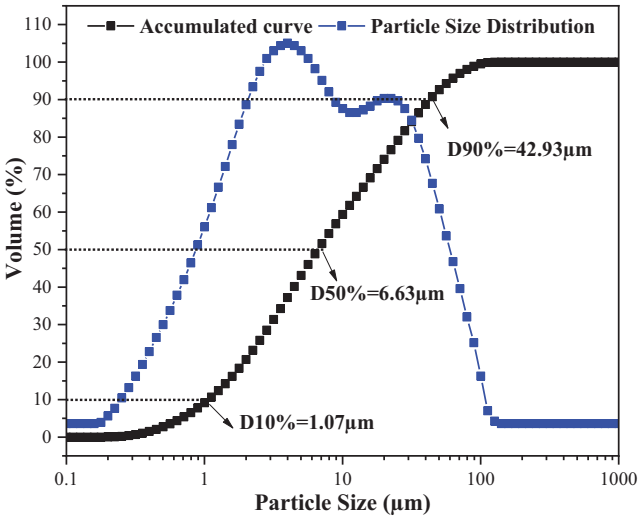

Fig. 6 Particle size distribution for the α-MoO_3 catalyst.

in this temperature range, shows a discrete endothermic peak around 788 °C, which is related to the orthorhombic crystalline phase melting point (α-MoO_3). The results commented on in this work are in according with the literature (Al-Alotaibi et al., 2021; Hou et al., 2018).

The oxides percentages present given by X-ray fluorescence (EDX) for the α-MoO_3 catalyst were (MoO_3) 99.57% and (Fe_2O_3) 0.43%. The EDX results confirm that molybdenum oxide is the majority element present in the catalyst obtained by combustion reaction, which corresponded to about 99% of the total, followed by discrete traces of iron oxide that accounted for about 0.43% possibly resulting from the preparation process by combustion reaction. The values expressed in this work corroborate with the studies of Sales et al. (2020), when they studied photocatalysts of MoO_3 obtained by a Pechini-based method and applied to effluent treatment.

The particle size analysis is graphically illustrated in Fig. 6, which express the distribution values of the equivalent particles spherical diameters as a function of the cumulative volume for the catalyst (α-MoO_3) obtained by combustion reaction.

Analyzing Fig. 6, it can be seen that the α-MoO_3 catalyst exhibits a polymodal particle size distribution curve with a wide range of size distributions. A concentration of particles between ~0.2 and 100 µm can be observed, and an average particle diameter of 15.43 µm is obtained. The accumulated values (black curve) illustrate a particle size accumulation of 1.07 µm up to 10%, 6.63 µm up to 50%, and 42.92 µm up to 90%. The particle size values observed in this work differ from recent published literature (Shahsank et al., 2021; Prakash et al., 2018; Rammal and Omanovic, 2020), which report a nanometer scale for powders obtained by similar methods, since in the present study the integrated synthesis method provided the formation of single phase MoO_3 during the process and with micrometric characteristics.

Fig. 7 illustrates the scanning electron microscopy results for the α-MoO_3 catalyst, synthesized by combustion reaction.

Looking at Fig. 7, the micrographs illustrate the morphological with well-defined appearance, oriented plates with directional growth preferences, what is corroborated by X-ray diffraction analysis, which showed that the catalyst is single phase with crystalline structure orthorhombic (α-MoO_3) (Rammal and Omanovic, 2020); and also having a wide distribution of sizes, as already observed by the analysis of granulometric distribution (Fig. 5). The morphological aspects of plaques obtained in this work are in agreement with the studies of Sales et al. (2020)), when they studied molybdenum trioxide with orthorhombic phase (α-MoO_3) synthesized by the Pechini method applied to photocatalysis and the research of Gangaraju et al. (2017), when they synthesized (α-MoO_3) by combustion reaction and applied to batteries.

The catalyst presented a value of 1.36 m^2g^{-1} for the surface area, a relatively low value, characteristic of MoO_3-based materials (Pinto et al., 2019), such behavior suggests that regardless of the Synthesis method, catalytic property and rel-

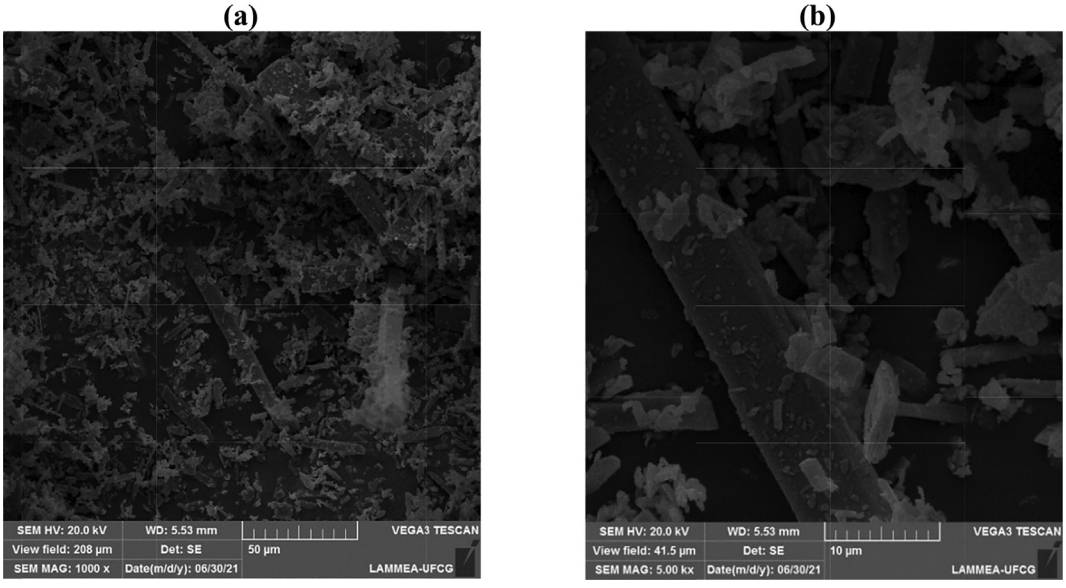

Fig. 7 Morphologies obtained by SEM for the α-MoO_3 catalyst, (a) 1000x; (b) 5000x.

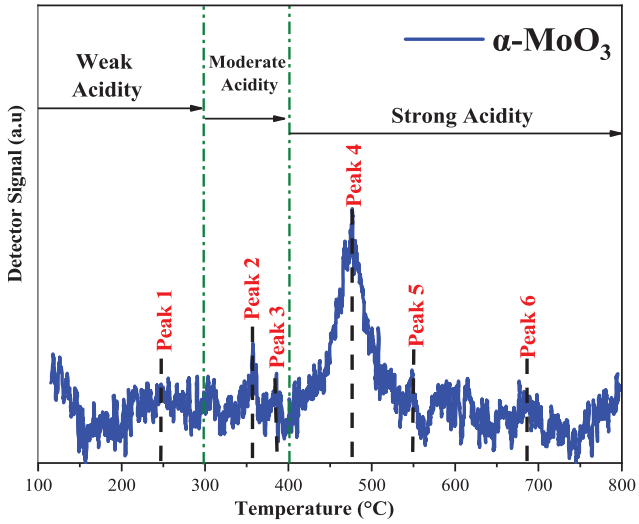

Fig. 8 TPD-NH_3 analysis of the α-MoO_3 catalyst α-MoO_3.

Table 3 Type of acidity present in catalyst (α-MoO_3).

Catalyst	Peak	Temperature (°C)	Acidity (μmol/g de NH_3)	Type of Acidity
(α-MoO_3)	1	246	3.33	Weak
	2	356	7.74	Moderate
	3	384	4.88	Moderate
	4	477	13.48	Strong
	5	547	2.65	Strong
	6	685	1.51	Strong
	Total acidity = 33.61 μmol/g de NH_3			

atively low surface areas are an intrinsic characteristic of this material (Sales et al., 2020).

The density for the α-MoO_3 catalyst evidenced by the He pycnometry test was 4.5 g/cm^3, a value that showed little deviation from the theoretical density revealed by the standard PDF2(2019) 00–005-0508, which is 4.71 g/cm^3, whose calculated relative error was 3.6%, thus illustrating the good proximity of the material produced in this work to the theoretical values. Concepts such as density are important, as the measurements allow defining the mass of solid catalyst that will be used in an industrial reactor (Dantas et al., 2021).

In the Fig. 8 presents the acidity data for the α-MoO_3 catalyst, obtained by thermo-programmed desorption (TPD-NH_3).

The parameters for acid characterization of the catalyst (α-MoO_3) were obtained based on the literature (Silva et al., 2020b; Lima and Perez-Lopez, 2018; Dantas et al., 2017) and are shown in the Table 3. They indicate that NH_3 thermodesorption peaks observed in regions at temperatures below 300 °C correspond to acid sites of weak nature, peaks between 300 and 400 °C correspond to acid sites of moderate nature, and peaks observed at temperatures above 400 °C are attributed to acid sites of strong nature.

According to Table 3, the α-MoO_3 catalyst presented six peaks of thermodesorption of NH_3 characteristics of the three types of acid strength (weak, moderate and strong), with predominance of moderate and strong acid sites. However, the total acidity of the catalyst was 33.61 μmol.g^{-1} of NH_3. The total acidity values presented in this work, are higher when compared to the work of Pinto et al. (2019), this can possibly be explained by the different synthesis method for MoO_3.

In this case, considering the surface area obtained in analysis (1.36 m_2g^{-1}) for α-MoO_3 catalyst, there is a distribution of acid sites is 24.71 μ.mol m^2. So, it can be concluded that the catalyst, obtained by pilot scale combustion reaction, exhibits acid sites, which can satisfactorily con-tribute to biodiesel production reactions.

Table 4 Planning response 2^2 obtained for the random variables temperature and catalyst quantity.

Experiment	(A) Temperature (°C)	(B) Catalyst (%)	Y = Average Conversion in Ester (%)
1	100	2	18.8
2	100	4	20.3
3	200	2	96.8
4	200	4	96.6
5	79.3	3	6.5
6	220.7	3	96.9
7	150	1.6	78.6
8	150	4.4	74.4
9 (C)*	150	3	80.8
10 (C)*	150	3	78.2
11 (C)*	150	3	80.0
12 (C)*	150	3	73.1

*(C) Central point, * Fixed conditions: 30 g oil mass, time 1 h, and alcohol/oil ratio (15:1).

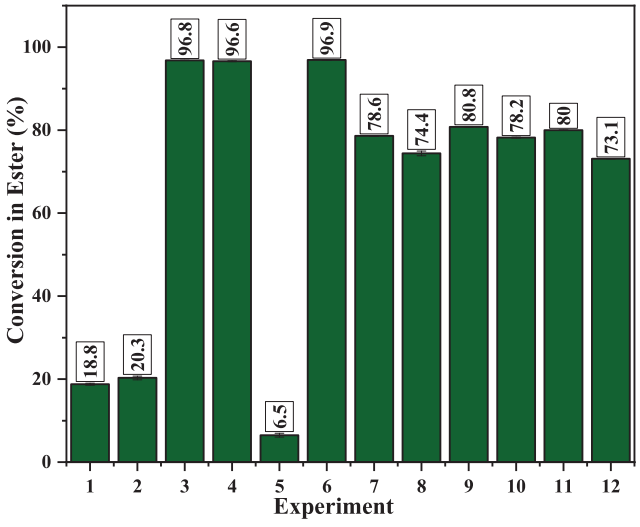

Fig. 9 Soybean oil conversion percentage results to ethyl esters obtained in the presence of the α-MoO_3 catalyst.

3.1. Performance of catalyst α-MoO_3

Table 4 describes the planning response used to analyze the statistical data for biodiesel production.

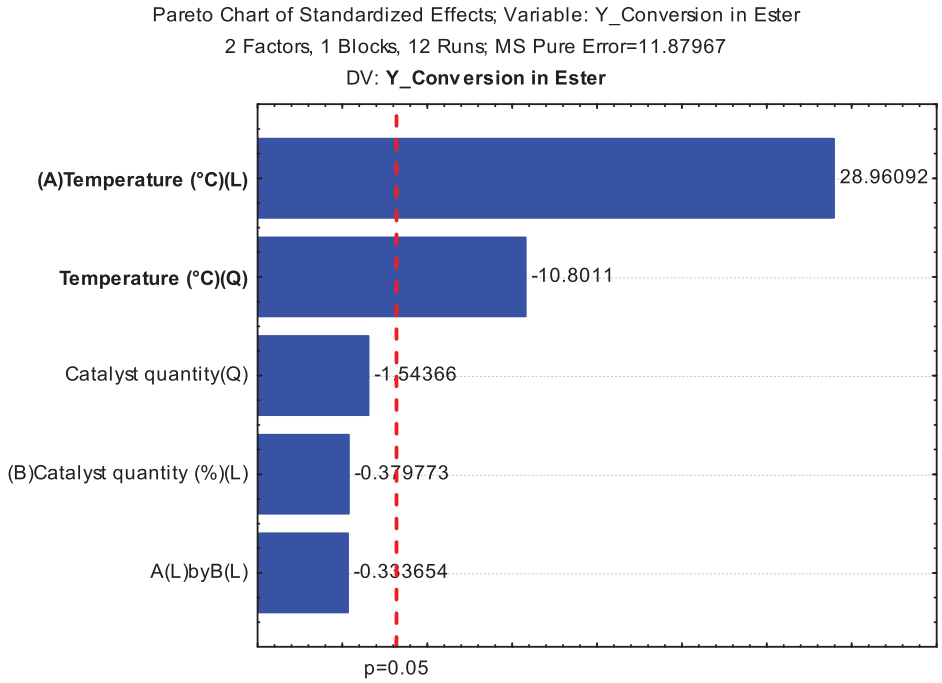

Fig. 10 Pareto chart resulting from the central composite factorial design 2^2 for the conversion of soybean oil into biodiesel.

In general, it could be observed (Table 4) that the α-MoO_3 catalyst was active and conversions into fatty acid esters ranging from 73 to 96% where reached when the temperatures used are equal to or greater than 150 °C. All ethyl ester conversion results obtained from the experimental design are also illustrated in Fig. 9.

The best catalytic activities were observed for experiments 3, 4 and 6, with emphasis on the axial point of the design (Experiment 6) with 96.9% conversion to esters when used at a temperature of 220.7 °C, amount of catalyst 3% and the fixed conditions 30 g oil mass, 1 h and alcohol/oil ratio 15:1.

It is important to emphasize that the conditions used in this work were mild compared to recent literature (Pinto et al., 2019; Xie and Zhao, 2014; Mohebbi et al., 2020). Notably, Pinto et al. (2019) used MoO_3 by mass as the active phase for biodiesel production; however, the authors also use harsh reaction conditions such as molar ratio of 90:1, 5% of catalyst and up to 8 h of reaction, obtaining conversions of up to 95% of soybean oil methyl esters.

It is also important to highlight that this work used the ethyl route, which is beneficial to the process since the alcohol used is obtained from a renewable source, such as sugar cane (Shikida and Bacha, 2019; Alves et al., 2021). The performance of the α-MoO_3 catalyst may be associated with the presence of strong acid sites (Pinto et al., 2019) (see Table 3), which gives the system great versatility, and high conversions into biodiesel. Furthermore, in previous studies the reuse of similar catalysts in the frying oil was tested, and the α-MoO_3 catalyst maintained catalytic activity for five reuse cycles, confirming the high potential of the catalyst developed for industrial applications (Silva et al., 2022). Considering the best ester conversions (Fig. 10 and Table 4), the acidity and kinematic viscosity indexes of biodiesel were obtained and the data are presented in Table 5.

Based on the data presented in Table 5 and with the results of conversions of biodiesels obtained from experiments 3, 4 and 6 (Fig. 9), it is possible to observe that are in accordance with the biodiesel quality parameters of the Brazilian regulatory standards (ANP N° 51 DE 25/11/2015) (ANP, 2008) and European (EN 14214) (EN - 14214, 2003), in which they are established the minimum ester contents of 96.5% (quantified by gas chromatography) and kinematic viscosity (at 40 °C) of 3.0–6.0 mm^2/s in addition to the maximum acidity index of 0.50 mg KOH/g.

Table 5 Acid value index and kinematic viscosity of the products of experiments 3, 4 and 6 related to the production of biodiesel.

Experiment	Acidity Index (mgKOH/g)	Kinematic viscosity at 40 °C (mm^2/s)
3	0.50 ± 0.15	5.94 ± 0.06
4	0.50 ± 0.01	5.88 ± 0.01
6	0.48 ± 0.01	5.84 ± 0.00

3.2. Statistical analysis

The Pareto graph (Fig. 10) was initially used for the statistical analysis of the experimental design response for the optimization of the conditions of the transesterification of soybean oil catalyzed by α-MoO_3.

It is possible to observe in Fig. 10, that among the variables, the most significant, both linear and quadratic, was the temperature with 95% reliability ($p < 0.05$), with a greater interference of the temperature linear variable for larger values, i.e., the positive level, in contrast to the quadratic behavior of the same variable, which had a negative influence. The catalyst quantity variable as well as the interactions between the variables showed no statistically significant effect. These observa-

tions corroborate with the data in Table 3 and Fig. 8, suggesting that the increase in reaction temperature, significantly increases the soybean oil conversion to biodiesel.

Level curves of the experimental design response were also obtained, using the independent variables: amount of catalyst (%) and temperature (°C) and is ilustrated in Fig. 11.

The effect of reaction temperature under the conversion of ethyl esters was best evaluated and for high levels of temperature (+1) (220 °C) and amount of catalyst (4.4%), the biodiesel conversion was maximum (close to 100%), corroborating what was observed in the Pareto chart (Fig. 10).

However, it was also possible to observe that when the reaction temperatures are lowered (reaction temperature is below 150 °C) for both catalyst percentages, the conversion to esters also decreases, while still remaining below 40%. Therefore, it can be inferred that the temperature variable is the most statistically significant to the process and showing excellent catalytic behavior for the α-MoO_3 acid catalyst.

In the region investigated, the response surface is satisfactorily described by the quadratic mathematical model given by Equation (3), which presented an R^2 of 98% and which defines the plane represented in perspective on the contour line (Fig. 11), from the experimental planning performed and which best represents the data collected and adjusted to the data in Table 3.

$$Y(x,y) = -183.06973776469 + 2.5062039912853 \times x - 0.0058862500000001 \times x^2 + 13.880963023967 \times y - 2.103125 \times y^2 - 0.0115 \times x \times y + 0 \quad (3)$$

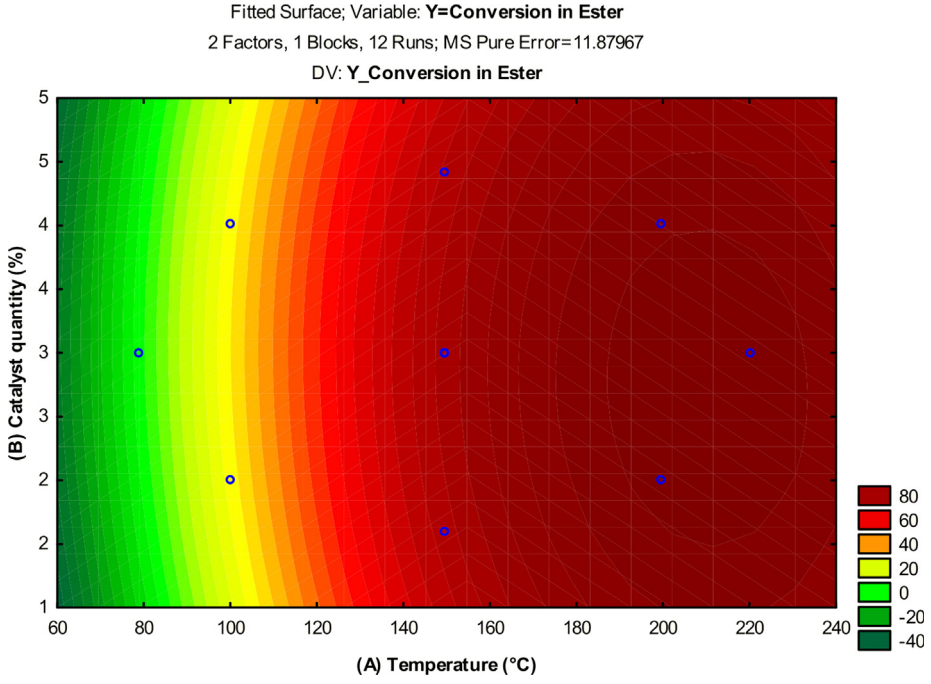

Fig. 11 Level curve for the soybean oil conversion to biodiesel with the interaction between (B) amount of catalyst (%) and (A) temperature (°C).

Table 6 ANOVA for optimizing biodiesel production from soybean oil using an acid catalyst α-MoO_3.

Variation Source	Quadratic Sum	Degree of Freedom	Quadratic Average	$F_{Calculed}$	F_{cal}/F_{tab}
Regression	11357.55	5	2271.51	69.40	15.82
Waste	196.38	6	32.73	–	–
Lack of Adjustment	160.74	3	53.58	4.51	0.49
Pure Error	35.64	3	11.88	–	–
Total	11553.93	11			
$F_{tabulated\ Regression}$	4.39	6			
$F_{tabulated\ Lack\ of\ Adjustment}$	9.28	9			
% Mx. Explained	98.30	–			
% Mx. Explainable	99.69	–			
R^2	0.98	–			
Fit Quality	0.76	–			
S (standard regression error)	5.72	–			

The data presented in Figs. 10 and 11 and the quadratic equation (Equation (3)), indicate that the model represents a relatively good description of the experimental data related to the ethyl ester content at the reaction time of 1 h, alcohol-oil ratio of 1/15, 3% catalyst and temperature of 220 °C, conditions revealed as optimal by the statistical model adopted. The quadratic model fit was also tested by analysis of variance (ANOVA) according to Table 6.

The ANOVA results (Table 6), showed a value for Fcal / Ftab of 15.82 for the regression, indicating that the model was statistically significant, and the value for Fcal / Ftab of the fit lack of 0.49 indicating that the model was predictive. Therefore, the regression model given by Equation (2) was a reasonable predictor of the experimental results, and the affected factors were real at a 95% confidence level, as already noted in Fig. 11.

4. Conclusions

The α-MoO_3 catalyst was successfully synthesized on a pilot scale using a combustion reaction. The pilot-scale production was safe, reproducible, and efficient. The synthesized catalyst is single-phase (α-MoO_3 orthorhombic), micrometric with an average particle size of (15.43 μm) and surface area (S_{BET} = 1.36 m^2g^{-1}). The use of central composite factorial planning made it possible to evaluate the process in a multivariate manner, leading to the identification of variables that significantly influenced the response variable (soybean oil conversion to esters). The factorial design allowed us to identify the influence of the variables (catalyst percentage and temperature) in the soybean oil transesterification. According to the statistical study, the temperature was the variable that most affected the value of the response variable, and the statistical model adopted was significant and predictive with a significance level of 95%. The catalyst was effective when the temperature was ~150 °C, showing ester conversions up to 96%, the acidity of the biodiesel produced ranged from 0.48 to 0.50 mg KOH/g and kinematic viscosity of 5.84–5.94 mm^2/s, with significantly promising results using ethanol as transesterification agent. From the results obtained, it can be concluded that the catalyst studied can be successfully applied in biodiesel production, since from its fast and easy preparation to the high conversions achieved outperform traditional methods, since this catalyst is a new material with innovative characteristics.

Declaration of Competing Interest

The authors declare that they have no known competing financial interests or personal relationships that could have appeared to influence the work reported in this paper.

Acknowledgments

This work was carried out with financial support from the Coordenação de Aperfeiçoamento de Pessoal de Nível Superior - CAPES and Conselho Nacional de Desenvolvimento Científico e Tecnológico CNPq Brazil Funding Code 001.

Open Access

References

Al-Alotaibi, A.L., Altamimi, N., Howsawi, E., Elsayed, K.A., Massoudi, I., Ramadan, A.E., 2021. Synthesis and Characterization of MoO_3 for Photocatalytic Applications. J. Inorg. Organomet. Polym Mater. 31, 2017–2029. https://doi.org/10.1007/s10904-021-01939-w.

Ali, O.M., Mamat, R., Najafi, G., Yusaf, T., Safieddin Ardebili, S.M., 2015. Optimization of Biodiesel-Diesel Blended Fuel Properties and Engine Performance with Ether Additive Using Statistical Analysis and Response Surface Methods. Energies. 8, 14136–14150. https://doi.org/10.3390/en81212420.

Alves, L.Q., Franco, P.N., Zanetti, W.A.L., Góes, B.C., 2021. Desempenho da produção da cultura de cana-de-açúcar nos principais estados produtores. Revista Brasileira de Engenharia de Biossistemas. 15, 303–317. https://doi.org/10.18011/bioeng2021v15n2p303-317.

American Society for Testing Meterials, U., 2000. ASTM D-445, Kinematic Viscosity of Transparent and Opaque Liquids.

American Society for Testing Materials, U. A., 2008. Determination of free and total glycerin in B100 biodiesel. Methyl esters by gas chromatography (GC). Designación D6584.

ANP. Agência Nacional do Petróleo, Gás Natural e Biocombustíveis. 2008, Brasil. Resolução no 7, de 19/03/2008. Regulamento Técnico ANP.

AOCS, A., 2017. Official Method Cd 3d-63. Acid Value of fats and oils.

Baez-Rodriguez, A., Zamora-Peredo, L., Alvarez-Fregoso, O., Martinez-Martinez, R., Huerta-Arcos, L., Falcony, C., Alvarez-Perez, M.A., Garcia-Hipolito, M., 2019. Effective photo- and cathodoluminescence from alpha-MoO_3:Eu^{3+} films obtained through the pyrosol method. J. Photonics Energy 9. https://doi.org/10.1117/1.jpe.9.046001.

Bergman, T.L., Lavine, A.S., Queiroz, E.M., 2000. Fundamentos de Transferência de Calor E de Massa. Grupo Gen-LTC.

Chandar, N.R., Agilan, S., Muthukumarasamy, N., Thangarasu, R., 2019. An enhanced photocatalytic performance based on MoO_3 and zn doped MoO_3 nano structures. J. Ovonic Res. 15, 287–299.

Costa, A., Kiminami, R., 2012. Dispositivo para produção de nanomateriais cerâmicos em larga escala por reação de combustão e processo contínuo de produção dos nanomateriais. Revista de Propriedade Industrial–RPI 25, 002181–002183.

Dantas, J., Leal, E., Mapossa, A.B., Cornejo, D.R., Costa, A.C.F.M., 2017. Magnetic nanocatalysts of $Ni_{0.5}Zn_{0.5}Fe_2O_4$ doped with Cu and performance evaluation in transesterification reaction for biodiesel production. Fuel 191, 463–471. https://doi.org/10.1016/j.fuel.2016.11.107.

Dantas, J., Leal, E., Mapossa, A.B., Pontes, J.R.M., Freitas, N.L., Fernandes, P.C.R., Costa, A.C.F.M., 2021. Biodiesel production on bench scale from different sources of waste oils by using NiZn magnetic heterogeneous nanocatalyst. Int. J. Energy Res. 45, 10924–10945. https://doi.org/10.1002/er.6577.

Dighore, N.R., Anandgaonker, P., Gaikwad, S.T., Rajbhoj, A.S., 2016. Green synthesis of 2-aryl benzothiazole heterogenous catalyzed by MoO_3 nanorods. Green Process. Synth, 5, 139–143. https://doi.org/10.1515/gps-2015-0065.

EN - 14214 - Automotive Fuels - Fatty Acid Methyl Esters (FAME) for Diesel, 2003.

Farias, A.F.F., de Araújo, D.T., Silva, A.L., Leal, E., Pacheco, J.G.A., Silva, M.R., Kiminami, R.H.G.A., Costa, A.C.F.M., 2020. Evaluation of the catalytic effect of ZnO as a secondary phase in the $Ni_{0.5}Zn_{0.5}Fe_2O_4$ system and of the stirring mechanism on biodiesel production reaction. Arabian J. Chem. 13, 5788–5799. https://doi.org/10.1016/j.arabjc.2020.04.016.

Gadamsetti, S., Mathangi, N., Hussain, S., Kumar Velisoju, V., Chary, K.V.R., 2018. Vapor phase esterification of levulinic acid catalyzed by γ-Al_2O_3 supported molybdenum phosphate catalysts. Molecular Catalysis. 451, 192–199. https://doi.org/10.1016/j.mcat.2018.01.011.

Gangaraju, V., Bhargavi, D., Rangappa, D., 2017. Synthesis and Characterization of α-MoO_3/RGO Composite as Anode Material for Li-Ion Batteries Using Spray Drying Combustion. Mater. Today:. Proc. 4, 12328–12332. https://doi.org/10.1016/j.matpr.2017.09.167.

Gonçalves, M.A., Mares, E.K.L., Zamian, J.R., da Rocha Filho, G. N., da Conceição, L.R.V., 2021. Statistical optimization of biodiesel production from waste cooking oil using magnetic acid heterogeneous catalyst $MoO_3/SrFe_2O_4$. Fuel 304,. https://doi.org/10.1016/j.fuel.2021.121463 121463.

He, L., Zhang, S., Chen, Y., Ren, L., Li, J., 2018. Techno-economic potential of a renewable energy-based microgrid system for a sustainable large-scale residential community in Beijing, China. Renewable Sustainable Energy Rev. 93, 631–641. https://doi.org/10.1016/j.renene.2019.07.092.

Hou, X., Huang, J., Liu, M., Li, X., Hu, Z., Feng, Z., Zhang, M., Luo, J., 2018. Single-Crystal MoO_3 Micrometer and millimeter belts prepared from discarded molybdenum disilicide heating elements. Sci. Rep. 8, 1–8. https://doi.org/10.1038/s41598-018-34849-y.

Hwang, C.-C., Tsai, J.-S., Huang, T.-H., Peng, C.-H., Chen, S.-Y., 2005. Combustion synthesis of Ni–Zn ferrite powder—influence of oxygen balance value. J. Solid State Chem. 178, 382–389. https://doi.org/10.1016/j.jssc.2004.10.045.

Jain, S., Adiga, K., Verneker, V.P., 1981. A new approach to thermochemical calculations of condensed fuel-oxidizer mixtures. Combust. Flame 40, 71–79. https://doi.org/10.1016/0010-2180(81)90111-5.

Klug, H. P., Alexander, L.E., 1974. X-ray diffraction procedures: for polycrystalline and amorphous materials.

Lima, D., Perez-Lopez, O., 2018. Catalytic conversion of ethanol over ZSM-5-supported catalysts. Cerâmica. 64, 1–9. https://doi.org/10.1590/0366-69132018643692143.

Maniruzzaman, M., Rahman, M.A., Jeong, K., Lee, J., 2014. MoO_3/Au/MoO_3-PEDOT:PSS multilayer electrodes for ITO-free organic solar cells. Mater. Sci. Semicond. Process. 27, 114–120. https://doi.org/10.1016/j.mssp.2014.06.034.

Mohebbi, S., Rostamizadeh, M., Kahforoushan, D., 2020. Effect of molybdenum promoter on performance of high silica MoO_3/B-ZSM-5 nanocatalyst in biodiesel production. Fuel 266. https://doi.org/10.1016/j.fuel.2020.117063.

Mushtaq, A., Hanif, M.A., Zahid, M., Rashid, U., Mushtaq, Z., Zubair, M., Moser, B.R., Alharthi, F.A., 2021. Production and Evaluation of Fractionated Tamarind Seed Oil Methyl Esters as a New Source of Biodiesel. Energies. 14, 7148. https://doi.org/10.3390/en14217148.

Muthamizh, S., Sengottaiyan, C., Jayavel, R., Narayanan, V., 2020. Facile Synthesis of Phase Tunable MoO_3 Nanostructures and Their Electrochemical Sensing Properties. J. Nanosci. Nanotechnol. 20, 2823–2831. https://doi.org/10.1166/jnn.2020.17456.

Nagyne-Kovacs, T., Studnicka, L., Lukacs, I.E., Laszlo, K., Pasierb, P., Szilagyi, I.M., Pokol, G., 2020. Hydrothermal Synthesis and Gas Sensing of Monoclinic MoO_3 Nanosheets. Nanomaterials. 10. https://doi.org/10.3390/nano10050891.

Navajas, A., Reyero, I., Jimenez-Barrera, E., Romero-Sarria, F., Llorca, J., Gandia, L.M., 2020. Catalytic Performance of Bulk and Al_2O_3-Supported Molybdenum Oxide for the Production of Biodiesel from Oil with High Free Fatty Acids Content. Catalysts. 10. https://doi.org/10.3390/catal10020158.

Pinto, B.F., Garcia, M.A.S., Costa, J.C.S., de Moura, C.V.R., de Abreu, W.C., de Moura, E.M., 2019. Effect of calcination temperature on the application of molybdenum trioxide acid catalyst: Screening of substrates for biodiesel production. Fuel 239, 290–296. https://doi.org/10.1016/j.fuel.2018.11.025.

Prakash, N.G., Dhananjaya, M., Narayana, A.L., Shaik, D.P.M.D., Rosaiah, P., Hussain, O.M., 2018. High Performance One Dimensional α-MoO_3 Nanorods for Supercapacitor Applications. Ceram. Int. 44, 9967–9975. https://doi.org/10.1016/j.ceramint.2018.03.032.

Rammal, M.B., Omanovic, S., 2020. Synthesis and characterization of NiO, MoO_3, and NiMoO4 nanostructures through a green, facile method and their potential use as electrocatalysts for water splitting. Mater. Chem. Phys. 255. https://doi.org/10.1016/j.matchemphys.2020.123570.

Ramos, M., Dias, A.P.S., Puna, J.F., Gomes, J., Bordado, J.C., 2019. Biodiesel production processes and sustainable raw materials. Energies. 12, 4408. https://doi.org/10.3390/en12234408.

Sales, H.B., Menezes, R.R., Neves, G.A., Souza, J.J.N., Ferreira, J.M., Chantelle, L., Menezes de Oliveira, A.L., Lira, H.D.L., 2020. Development of Sustainable Heterogeneous Catalysts for the Photocatalytic Treatment of Effluents. Sustainability. 12, 7393. https://doi.org/10.3390/su12187393.

Sangeetha, D.N., Bhat, D.K., Selvakumar, M., 2019. h-MoO_3/Activated carbon nanocomposites for electrochemical applications. Ionics 25, 607–616. https://doi.org/10.1007/s11581-018-2684-2.

Santamaria, L., Beirow, M., Mangold, F., Lopez, G., Olazar, M., Schmid, M., Li, Z., Scheffknecht, G., 2021. Influence of temperature on products from fluidized bed pyrolysis of wood and solid recovered fuel. Fuel 283,. https://doi.org/10.1016/j.fuel.2020.118922 118922.

Santos, T.V., Santos Brainer, N., Amorin Pryston, D.B., Silva Avelino, D.O., Dornelas, C.B., Meneghetti, M.R., Meneghetti, S. M.P., 2019. Study of Neat and Mixed Sn (IV) and Mo (VI) Oxides for Transesterification and Esterification: Influence of the Substrate on Leaching. Catalysis Lett. 149, 3132–3137. https://doi.org/10.1007/s10562-019-02869-6.

Sen, S.K., Dutta, S., Khan, M.R., Manir, M.S., Dutta, S., Al Mortuza, A., Razia, S., Hakim, M.A., 2019. Characterization and Antibacterial Activity Study of Hydrothermally Synthesized h-MoO_3 Nanorods and alpha-MoO_3 Nanoplates. Bionanoscience. 9, 873–882. https://doi.org/10.1007/s12668-019-00671-7.

Shadidi, B., Alizade, H.H.A., Najafi, G., 2020. Performance and exergy analysis of a diesel engine run on petrodiesel and biodiesel blends containing mixed CeO_2 and MoO_3 nanocatalyst. Biofuels. 1–7. https://doi.org/10.1080/17597269.2020.1779976.

Shahsank, M., Bhojya Naik, H.S., Sumedha, H.N., Nagaraju, G., 2021. Implementing an in-situ carbon formation of MoO_3 nanoparticles for high performance lithium-ion battery. Ceram. Int. 47, 10261–10267. https://doi.org/10.1016/j.ceramint.2020.07.241.

Shikida, P.F.A., Bacha, C.J.C., 2019. Aspectos Economicos da Geraçao de Tecnologia e a Utilização dos Principais Produtos e Subprodutos da Agroindústria Canavieira do Brasil. Revista de Economia e Sociologia Rural. 36, 9–30.

Silva, Farias, A.F.F., Pontes, J.R.M., Rodrigues, A.M., Costa, A.C.F. M., 2020a. Synthesis of the ZnO-$Ni_{0.5}Zn_{0.5}Fe_2O_4$-Fe_2O_3 magnetic catalyst in pilot-scale by combustion reaction and its application on the biodiesel production process from oil residual. Arabian Journal of Chemistry. 13, 7665–7679. https://doi.org/10.1016/j.arabjc.2020.09.003.

Silva, A.L., Farias, A.F.F., de Melo, J., Rodrigues, A.M., Meneghetti, S.M.P., Costa, A., 2022. Synthesis of MoO_3 by pilot-scale combustion reaction and evaluation in biodiesel production from residual oil. Int. J. Energy Res. 46, 7775–7787. https://doi.org/10.1002/er.7679.

Silva, Luna, C.B.B., Farias, A.F.F., Medeiros, S.A.S.L., Meneghetti, S.M.P., Rodrigues, A.M., Costa, A.C.F.M., 2020b. From Disposal to Reuse: Production of Sustainable Fatty Acid Alkyl Esters Derived from Residual Oil Using a Biphasic Magnetic Catalyst. Sustainability. 12. https://doi.org/10.3390/su122310159.

Song, Y.H., Zhao, Y., Huang, Z.F., Zhao, J.Z., 2017. Aqueous synthesis of molybdenum trioxide (h-MoO_3, alpha-MoO_3 center dot H_2O and h-/alpha-MoO_3 composites) and their photochromic properties study. J. Alloy. Compd. 693, 1290–1296. https://doi.org/10.1016/j.jallcom.2016.10.092.

Wang, Q., Wenlei, X., Guo, L., 2022. Molybdenum and zirconium oxides supported on KIT-6 silica: A recyclable composite catalyst for one–pot biodiesel production from simulated low-quality oils. Renewable Energy 187, 907–922. https://doi.org/10.1016/j.renene.2022.01.122.

Xie, W., Wan, F., 2019. Immobilization of polyoxometalate-based sulfonated ionic liquids on UiO-66-2COOH metal-organic frameworks for biodiesel production via one-pot transesterification-esterification of acidic vegetable oils. Chem. Eng. J. 365, 40–50. https://doi.org/10.1016/j.cej.2019.02.016.

Xie, W., Wang, H., 2020. Immobilized polymeric sulfonated ionic liquid on core-shell structured Fe_3O_4/SiO_2 composites: A magnetically recyclable catalyst for simultaneous transesterification and esterifications of low-cost oils to biodiesel. Renewable Energy 145, 1709–1719. https://doi.org/10.1016/j.renene.2019.07.092.

Xie, W., Zhao, L., 2014. Heterogeneous CaO–MoO_3–SBA-15 catalysts for biodiesel production from soybean oil. Energy Convers. Manage. 79, 34–42. https://doi.org/10.1016/j.enconman.2013.11.041.